

NEUTRON TRANSVERSITY AT JEFFERSON LAB

J. P. CHEN

Jefferson Lab, Newport News, VA 23606, USA

E-mail: jpchen@jlab.org

X. JIANG

Rutgers University, Piscataway, NJ 08855, USA

J.-C. PENG, L. ZHU

University of Illinois, Urbana, IL 61801, USA

FOR THE JEFFERSON LAB HALL A COLLABORATION

Nucleon transversity and single transverse spin asymmetries have been the recent focus of large efforts by both theorists and experimentalists. On-going and planned experiments from HERMES, COMPASS and RHIC are mostly on the proton or the deuteron. Presented here is a planned measurement of the neutron transversity and single target spin asymmetries at Jefferson Lab in Hall A using a transversely polarized ^3He target. Also presented are the results and plans of other neutron transverse spin experiments at Jefferson Lab. Finally, the factorization for semi-inclusive DIS studies at Jefferson Lab is discussed.

1. Introduction

After forty years of extensive experimental and theoretical efforts, the unpolarized Parton Distribution Functions (PDFs) have been extracted from DIS, Drell-Yan and other processes with excellent precision over a large range of x . The comparison of the structure functions in a large range of Q^2 with QCD evolution equations have provided one of the best tests of QCD. Since the “proton spin crisis” in the 1980s, very active spin-physics program have been carried out at CERN, SLAC and HERA, and, recently, at JLab and RHIC. Longitudinally polarized parton distribution functions have been extracted by a number of groups in recent years, although the precision is not as good as that of the unpolarized PDFs. The other equally important parton distribution functions, the transversity distributions, have only been explored recently.

1.1. *Transversity*

The transversity distributions, $\delta q(x, Q^2)$, are fundamental leading-twist (twist-2) quark distributions, same as the unpolarized and polarized parton distributions, $q(x, Q^2)$ and $\Delta q(x, Q^2)$. In quark-parton models, they describe the net transverse polarization of quarks in a transversely polarized nucleon¹. There are several special features for the transversity distributions, making them uniquely interesting:

- The difference between the transversity and the longitudinal distributions is purely due to relativistic effects. In the absence of relativistic effects (as in the non-relativistic quark model, where boosts and rotations commute), the transversity distributions are identical to the longitudinally polarized distributions.
- The quark transversity distributions do not mix with gluonic effects² and therefore follow a much simpler evolution and have a valence-like behavior.
- The positivity of helicity amplitudes leads to the Soffer's inequality for the transversity³: $|h_1^q| \leq \frac{1}{2}(f_1^q + g_1^q)$.
- The lowest moment of h_1^q measures a simple local operator analogous to the axial charge, known as the "tensor charge", which can be calculated from lattice QCD.

Due to the chiral-odd nature of the transversity distribution, it can not be measured in inclusive DIS experiments. In order to measure $\delta q(x, Q^2)$, an additional chiral-odd object is required, such as double-spin asymmetries in Drell-Yan processes, single target spin azimuthal asymmetries in Semi-Inclusive DIS reactions, double-spin asymmetries in Λ production from e-p and p-p reactions and single-spin asymmetries in double pion production from e-p scattering. The first results, from measurements performed by the HERMES⁴ and COMPASS⁵ collaborations with SIDIS offered the first glimpse of possible effects caused by the transversity distributions.

1.2. *Semi-Inclusive Deep-Inelastic-Scattering*

Semi-inclusive DIS is a powerful tool for probing various parton distributions and fragmentation functions. For producing a spin-zero meson, the SIDIS differential cross section at leading order contains 8 structure functions^{6,7}. The single transverse target spin asymmetry term contains the Collins term⁸, which contains the product of the transversity and the Collins fragmentation function and is proportional to $\sin(\phi_h^\ell + \phi_S^\ell)$, the

Sivers term⁹, which contains the product of the Sivers structure function with the regular fragmentation function and is proportional to $\sin(\phi_h^\ell - \phi_s^\ell)$, and a third term proportional to $\sin(3\phi_h^\ell - \phi_s^\ell)$. Azimuthal angles are defined relative to the lepton plane, e.g. $\phi_h^\ell = \phi_h - \phi^\ell$ is the angle between the hadron plane and the lepton plane and $\phi_s^\ell = \phi_s - \phi^\ell$ is the angle between the spin plane and the lepton plane. SIDIS can be used to extract all eight of the twist-2 structure functions by choosing different beam helicity and target polarization configurations, and detecting the azimuthal angular dependences (ϕ_h^l and ϕ_s^l).

1.3. *Experimental Status*

The HERMES collaboration reported two years ago the observation of single-spin azimuthal asymmetries for charged and neutral hadron electroproduction¹⁰. Using an unpolarized positron beam on longitudinally polarized hydrogen and deuterium targets, the cross section was found to have a $\sin\phi_h^l$ dependence. Although a longitudinally polarized target was used in the HERMES experiment, there is a small (≈ 0.15) nonzero value of polarization transverse to the virtual photon direction. The observed azimuthal asymmetries arise from Collins, Sivers and higher-twist contributions from the longitudinal target polarization. For a longitudinally polarized target ($\phi_s^l = 0$) the Collins and the Sivers mechanisms can not be distinguished.

If the azimuthal asymmetry observed by HERMES is indeed partially caused by the nucleon transversity, a much larger asymmetry is expected for a transversely polarized target. The HERMES⁴ and COMPASS⁵ collaborations have collected polarized SIDIS data using transversely polarized hydrogen and LiD targets, respectively. A simultaneous fit to $\sin(\phi_h^l + \phi_s^l)$ and $\sin(\phi_h^l - \phi_s^l)$ dependences was applied to the HERMES data to extract the ‘‘Collins moments’’ and the ‘‘Sivers moments’’, respectively. Nonzero Collins moments were clearly observed in the HERMES data with positive azimuthal asymmetry for π^+ and negative azimuthal asymmetry for π^- . The unexpectedly large magnitude for the azimuthal asymmetry of π^- relative to π^+ seems to suggest that the disfavored Collins function is of comparable magnitude, but opposite sign, to the favored Collins function. Furthermore, the observation of the $\sin(\phi_h^l - \phi_s^l)$ moments shows that the Sivers function is nonzero and indeed contributes to the azimuthal asymmetry in SIDIS. Preliminary results⁵ from the COMPASS 2002 data show that the $\sin(\phi_h^l + \phi_s^l)$ azimuthal asymmetry is consistent with zero for a

transversely polarized LiD target. A factor of 4 increase in statistics is expected for the COMPASS 2002-2004 data.

To be able to extract the transversity from the Collins moments, independent measurements of the Collins fragmentation functions are needed. First results of an extraction of the Collins fragmentation functions from $e^+ + e^-$ measurements by the Belle collaboration at KEK is available now¹¹.

2. A planned measurement of neutron transversity at JLab

The Thomas Jefferson National Accelerator Facility (Jefferson Lab, or JLab) produces a continuous-wave electron beam of energy up to 6 GeV. An energy upgrade to 12 GeV is planned in the next few years. The electron beam with a current up to 180 μA is polarized up to 85% by illuminating a strained GaAs cathode with polarized laser light. The electron beam goes into three experimental halls (Halls A, B and C) where the electron scattering off various nuclear targets takes place. The experiments reported here studied semi-inclusive (or inclusive) electron scattering where the scattered electron and one scattered hadron (or only the scattered electron) are detected. The neutron experiments presented here are from Hall A¹² where a polarized ^3He target, with in-beam polarization of about 40%, provides an effective polarized neutron target. The polarized luminosity reached is $10^{36} \text{ s}^{-1} \text{ cm}^{-2}$. There are two High Resolution Spectrometers (HRS) with momentum up to 4 GeV/c. The HRS detector package consisted of vertical drift chambers (for momentum analysis and vertex reconstruction), scintillation counters (data acquisition trigger) and particle identification detectors: gas Čerenkov counters and lead-glass calorimeters for electron detection or Aerogel and heavy gas Čerenkov detectors and RICH detectors for hadron particle identification. In addition to the HRS's, the BigBite spectrometer with a large acceptance is used for detecting electrons for the semi-inclusive experiments where large acceptance is needed. The BigBite detector package consists of drift chambers, scintillators and a lead-glass calorimeter.

A recently approved JLab proposal¹³ plans to measure the single-spin asymmetry of the $\vec{n}(e, e'\pi^-)X$ reaction on a transversely polarized ^3He target. The goal of this experiment is to provide the first measurement of the neutron transversity, complementary to the ongoing HERMES and COMPASS measurements on the proton and deuteron. This experiment focuses on the valence quark region, $x = 0.19 - 0.34$, at $Q^2 = 1.77 - 2.73 \text{ GeV}^2$. Data from this experiment, when combined with data from HER-

MES and COMPASS, will provide powerful constraints on the transversity distributions of both u -quarks and d -quarks in the valence region.

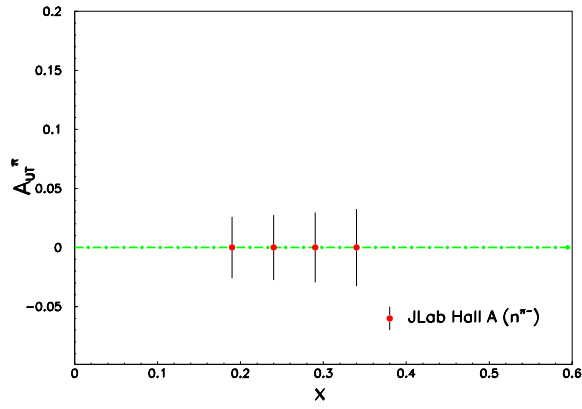


Figure 1. Expected statistical precision of this experiment .

The experiment will use a 6 GeV electron beam with the Hall A left-side high resolution spectrometer (HRS_L) situated at 16° as the hadron arm, and the BigBite spectrometer located at 30° beam-right as the electron arm. A set of vertical coils will be added to the polarized ^3He target to provide tunable polarization directions in all three dimensions. By rotating the target polarization direction in the transverse plane, the coverage in ϕ_s^l is increased, hence facilitating the separation of the Collins and the Sivers effects. Figure 2 shows the expected statistical precision of this experiment with 24 days of beamtime for $\vec{n}(e, e'\pi^-)X$ single spin asymmetry. Due to the good particle identification in the HRS, K^- data will be collected at the same time, providing a set of precision data to study the transverse spin asymmetries for semi-inclusive K^- production.

The same measurement can be performed with the HRS spectrometer in positive polarity to detect π^+ and K^+ . A new proposal is being developed for this measurement.

3. Inclusive neutron transverse spin experiments at JLab

In addition to the transverse spin SIDIS experiments to study transversity, inclusive transverse spin experiments can be used to study higher-twist effects. There are several completed inclusive (double) transverse

spin experiments^{14,15,16} which precisely measured the second spin structure function g_2 and its moment d_2 . g_2 , unlike g_1 and F_1 , can not be interpreted in a simple quark-parton model. To understand g_2 properly, it is best to start with the operator product expansion (OPE) method. In the OPE, neglecting quark masses, g_2 can be cleanly separated into a twist-2 and a higher-twist term:

$$g_2(x, Q^2) = g_2^{WW}(x, Q^2) + g_2^{H.T.}(x, Q^2). \quad (1)$$

The leading-twist term, g_2^{WW} , can be determined from g_1 ¹⁷ and the higher-twist term arises from the quark-gluon correlations. Therefore g_2 provides a clean way to study higher-twist effects. In addition, at high Q^2 , the x^2 -weighted moment, d_2 , is a twist-3 matrix element and is related to the color polarizabilities¹⁸. Predictions for d_2 exist from various models and lattice QCD.

A precision measurement of g_2^n from JLab E97-103¹⁴ covered the Q^2 range from 0.58 to 1.36 GeV^2 at $x \approx 0.2$. Results for g_2^n are given on the left panel of Fig. 2. The light-shaded area in the plot gives the leading-twist contribution, obtained by fitting world data²⁰ and evolving to the Q^2 values of this experiment. The systematic errors are shown as the dark-shaded area near the horizontal axis.

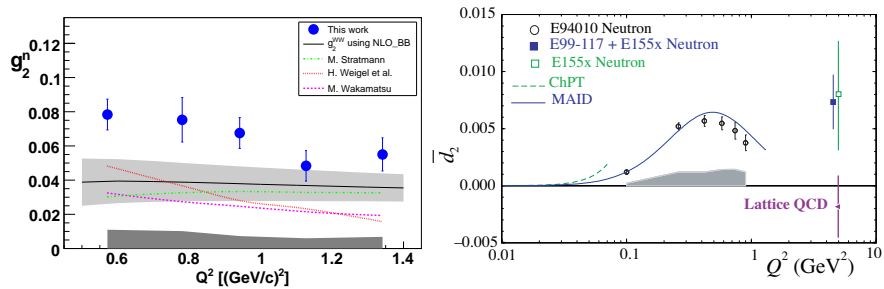


Figure 2. Results for g_2^n (left) and d_2^n (right) from JLab Hall A.

The precision reached is more than an order of magnitude improvement over that of the best world data¹⁹. The difference of g_2 from the leading twist part (g_2^{WW}) is due to higher twist effects. The measured g_2^n values are consistently higher than g_2^{WW} . For the first time, there is a clear indication that higher-twist effects become significantly positive at Q^2 below 1 GeV^2 ,

while the bag model²¹ and Chiral Soliton model^{22,23} predictions of higher-twist effects are negative or close to zero.

The second moment of the spin structure function, d_2 , can be extracted from g_1 and g_2 measurements. Due to x^2 weighting, the contributions are dominated by the high- x region and the problem of low- x extrapolation is avoided. The Hall A experiment E99-117¹⁵ provided data on A_2^n at high- x . Combining these results with the world data¹⁹, the second moment d_2^n was extracted at an average Q^2 of 5 GeV². This result is compared to the previously published result¹⁹ and a calculation by Lattice QCD²⁴. While a negative or near-zero value was predicted by Lattice QCD and most models, the new result for d_2^n is positive. Also shown in Fig. 2 are the low Q^2 (0.1-1 GeV²) results of the inelastic part of d_2^n from another Hall A experiment E94-010^{16,25}, which were compared with a Chiral Perturbation Theory calculation²⁶ and a model prediction²⁷.

4. Experimental Tests of Factorization for SIDIS at JLab

Due to the limitation of maximum beam energy (6 GeV now and 12 GeV after the planned energy upgrade), how well factorization works for SIDIS at JLab is an important issue. Due to the high luminosity, it is possible to select kinematical settings keeping Q^2 reasonably large by going to large scattering angles. With an optimal choice of kinematics, the typical SIDIS measurements at JLab will be at Q^2 around 2 GeV² with W^2 of 4-10 GeV² and W'^2 of around 4 GeV² for an x range of 0.1-0.4 and a z range of 0.4-0.6. At what precision level factorization will work can only be answered by experimental tests. First test results are becoming available from $p(e, e' \pi^{+-})$ experiments at JLab Hall C²⁸ and Hall B²⁹. These results show that at the 10% level, the data are consistent with the factorization assumption.

A JLab Hall A proposal³⁰ has been conditionally approved to measure unpolarized ($e, e' \pi^\pm$) and ($e, e' K^\pm$) reactions. The new data will provide further precision tests of factorization. In addition, the pion SIDIS measurement aims to determine $\bar{d} - \bar{u}$ with much better statistical accuracy than the existing HERMES data³¹, which will provide a complementary measurement of the sea asymmetry to the Drell-Yan process³².

Acknowledgments

This work is supported by the U.S. Department of Energy (DOE). The Southeastern University Research Association operates the Thomas Jefferson National Accelerator Facility for DOE under contract DE-AC05-

84ER40150, Modification No. 175.

References

1. V. Barone, A. Drago and P. Ratcliffe, Phys. Rep. **359**, 1 (2002).
2. C. Bourrely, J. Soffer and O. V. Teryaev, Phys. Lett. **B420**, 375 (1998).
3. J. Soffer, Phys. Rev. Lett. **74**, 1292 (1995).
4. M. Diefenthaler, Proceedings of DIS2005, AIP **792**, 933 (2005).
5. P. Pagano, Proceedings of DIS2005, AIP **792**, 937 (2005).
6. P. Mulders and R. D. Tangerman, Nucl. Phys. **B461**, 197 (1996).
7. D. Boer and P. Mulders, Phys. Rev. **D57** 5780, (1998).
8. J. Collins, Nucl. Phys. **B396**, 161 (1993).
9. D. W. Sivers, Phys. Rev. **D41**, 83 (1990).
10. A. Airapetian, *et al.*, Phys. Lett. **B562**, 182 (2003).
11. A. Ogawa, *et al.*, Proceedings of DIS2005, AIP **792**, 949 (2005).
12. Hall A collaboration: J. Alcorn *et al.*, Nucl. Inst. Meth. **A522**, 294 (2004).
13. JLab E03-004, J. P. Chen, X. Jiang and J.-C. Peng, spokespersons; J. -C. Peng, *et al.*, Proceedings of HiX2004, AIP **747**, 141 (2004).
14. K. Kramer, *et al.*, Phys. Rev. Lett. **95**, 142002 (2005).
15. X. Zheng, *et al.*, Phys. Rev. Lett. **92**, 012004 (2004); X. Zheng, *et al.*, Phys. Rev. C **70**, 065207 (2004).
16. M. Amarian, *et al.*, Phys. Rev. Lett. **89**, 242301 (2002); *ibid.*, **92**, 022301 (2004); *ibid.*, **93**, 152301 (2004); Z. E. Meziani *et al.*, Phys. Lett. **B 613**, 148 (2005).
17. S. Wandzura and F. Wilczek, Phys. Lett. B **72** (1977).
18. X. Ji and W. Melnitchouk, Phys. Rev. **D 56**, 1 (1997).
19. K. Abe, *et al.*, E155 collaboration, Phys. Lett. **B493**, 19 (2000).
20. J. Blümlein and H. Bottcher, Nucl. Phys. **B636**, 225 (2002).
21. M. Stratmann, Z. Phys. **C 60**, 763 (1993).
22. H. Weigel, Pramana **61**, 921 (2003).
23. M. Wakamatsu, Phys. Lett. **B 487**, 118 (2000).
24. M. Gockeler *et al.*, Phys. Rev. **D 63**, 074506 (2001).
25. J. P. Chen, A. Deur and Z. E. Meziani, to appear in Mod. Phys. Lett. A (2005); nucl-ex/0509007.
26. X. Ji, C. Kao, and J. Osborne, Phys. Lett. B **472**, 1 (2000); C. W. Kao, T. Spitzenberg and M. Vanderhaeghen, Phys. Rev. D **67**, 016001 (2003); V. Bernard, T. Hemmert and Ulf-G. Meissner, Phys. Rev. D **67**, 076008
27. D. Drechsel, S. Kamalov and L. Tiator, Phys. Rev. D **63**, 114010 (2001).
28. JLab E00-108, R. Ent, H. Mkrtchyan and G. Niculescu, spokespersons; W. Melnitchouk, R. Ent and C. E. Keppel, Phys. Rept. **406**, 127 (2005).
29. H. Avagyan, a contribution to these proceedings.
30. JLab E04-114, J. P. Chen, X. Jiang, J.-C. Peng and L. Zhu, spokespersons (2004).
31. K. Ackerstaff, *et al.*, Phys. Rev. Lett. **81**, 5519 (1998).
32. G. T. Garvey and J. C. Peng, Prog. Part. Nucl. Phys. **47**, 203 (2001).